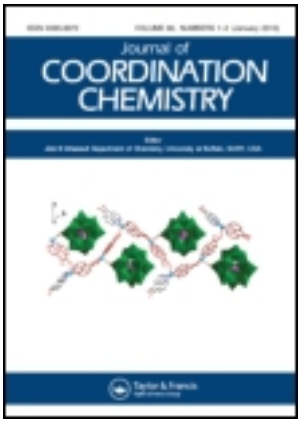

Journal of Coordination Chemistry
Publication details, including instructions for authors and subscription information:
http://www.tandfonline.com/loi/gcoo20

Synthesis, structural characterization, and antibacterial activity of mononuclear cobalt(III) azido complexes of two pentadentate Schiff bases derived from 2-hydroxynaphthaldehyde

Farzaneh Fadaee [a d], Mehdi Amirnasr [a], Azadeh Amirnasr [b], Kurt Mereiter [c] & Kurt Schenk-Joß [d]

[a] Department of Chemistry, Isfahan University of Technology, Isfahan, Iran

[b] Faculty of Science, Department of Biology, University of Isfahan, Isfahan, Iran

[c] Faculty of Chemistry, Vienna University of Technology, Vienna, Austria

[d] CCC-IPSB, École Polytechnique Fédérale de Lausanne, BSP Dorigny, Lausanne, Switzerland

Accepted author version posted online: 07 Mar 2013.Version of record first published: 10 Apr 2013.

To cite this article: Farzaneh Fadaee , Mehdi Amirnasr , Azadeh Amirnasr , Kurt Mereiter & Kurt Schenk-Joß (2013): Synthesis, structural characterization, and antibacterial activity of mononuclear cobalt(III) azido complexes of two pentadentate Schiff bases derived from 2-hydroxynaphthaldehyde, Journal of Coordination Chemistry, 66:8, 1363-1373

To link to this article: http://dx.doi.org/10.1080/00958972.2013.781159

Journal of Coordination Chemistry, 2013
http://dx.doi.org/10.1080/00958972.2013.781159

Synthesis, structural characterization, and antibacterial activity of mononuclear cobalt(III) azido complexes of two pentadentate Schiff bases derived from 2-hydroxynaphthaldehyde

FARZANEH FADAEE†¶, MEHDI AMIRNASR*†, AZADEH AMIRNASR‡, KURT MEREITER§ and KURT SCHENK-JOß¶

†Department of Chemistry, Isfahan University of Technology, Isfahan, Iran
‡Faculty of Science, Department of Biology, University of Isfahan, Isfahan, Iran
§Faculty of Chemistry, Vienna University of Technology, Vienna, Austria
¶CCC-IPSB, École Polytechnique Fédérale de Lausanne, BSP Dorigny, Lausanne, Switzerland

(*Received 13 September 2012; in final form 19 December 2012*)

The structural, spectroscopic, and electrochemical properties of [Co{(naph)$_2$dien}(N$_3$)] and [Co{(naph)$_2$dpt}(N$_3$)], where (naph)$_2$dien = bis-(2-hydroxy-1-naphthaldimine)-N-diethylenetriaminedianion and (naph)$_2$dpt = bis-(2-hydroxy-1-naphthaldimine)-N-dipropylenetriaminedianion have been investigated. These complexes are characterized by elemental analyses, IR, and UV–Vis spectroscopy. The crystal structures of these complexes have been determined by X-ray diffraction. The geometry around cobalt is distorted octahedral. The electrochemical behavior of these complexes in acetonitrile solution was also investigated. Both complexes show an irreversible Co^{III}–Co^{II} reduction at ca. −0.8 V, accompanied by dissociation of the axial Co^{II}–N$_3$ bond. The *in vitro* antibacterial activities of these complexes were tested against *Staphylococcus aureus* and *Bacillus licheniformis*.

Keywords: Cobalt(III) azido complexes; Pentadentate Schiff base ligand; Electrochemistry; Crystal structure; Antibacterial activity

1. Introduction

Study of mono-, di-, and polynuclear complexes of cobalt has been of interest for synthetic, structural, spectroscopic, magnetic, and optoelectronic features [1–5]. Schiff bases are useful chelators due to their ease of preparation, structural diversity, varied denticities, and subtle steric and/or electronic effects [6]. Pseudohalides such as azide have long been known for versatile coordination modes, leading to mononuclear, dinuclear, and polynuclear compounds [7]. Azide containing compounds are inhibitors for several enzymes, such as ATPases [8], so metal azido complexes [9, 10] are important for

*Corresponding author. Email: amirnasr@cc.iut.ac.ir

understanding their role in biological processes. The coordination mode of azide depends on the nature and oxidation state of the central metal ion as well as the nature of other coordinating ligands [11].

In continuation of our work on the synthesis and structural studies of transition metal complexes of pentadentate Schiff bases [12–14], herein we report the synthesis and spectroscopic characterization of [Co{(naph)$_2$dien}(N$_3$)] and [Co{(naph)$_2$dpt}(N$_3$)]. X-ray crystal structures are reported and cyclic voltammetric behavior and preliminary antibacterial activity of both complexes are also discussed.

2. Experimental

2.1. *Materials and general methods*

All solvents and chemicals were of commercial reagent grade and used as received from Aldrich and Merck. Elemental analyses were performed by using a Perkin–Elmer 2400II CHNS–O elemental analyzer. Infrared spectra (KBr pellets) were recorded on a FT-IR JASCO 680 instrument. Electronic spectra were obtained on a JASCO V-570 spectrophotometer. The redox properties of the complexes were studied by cyclic voltammetry. Cyclic voltammograms were recorded by using a SAMA 500 Research Analyzer. Three electrodes were utilized in this system, a glassy carbon working electrode, a platinum disk auxiliary electrode and a silver wire as reference electrode. The glassy carbon working electrode (Metrohm 6.1204.110) with 2.0 ± 0.1 mm diameter was manually cleaned with 1 μm alumina polish prior to each scan. Tetrabutylammonium hexafluorophosphate (TBAH) was used as supporting electrolyte. Acetonitrile was dried over CaH_2. The solutions were deoxygenated by purging with Ar for 5 min. All electrochemical potentials were calibrated *versus* internal $Fc^{+/0}$ ($E^0 = 0.4$ V *versus* Saturated Calomel Electrode) couple under the same conditions [15]v.

2.2. *Synthesis*

2.2.1. Synthesis of ligands. H_2(naph)$_2$dien and H_2(naph)$_2$dpt were prepared as reported in the literature [14].

2.2.2. Synthesis of [Co{(naph)$_2$dien}(N$_3$)] (1). To a stirring solution of $Co(CH_3COO)_2{\cdot}4H_2O$ (249 mg, 1 mM) in methanol (25 mL) was added an equimolar amount of the H_2(naph)$_2$dien (411 mg, 1 mM). The pink solution turned brown immediately due to formation of [Co^{II}{(naph)$_2$dien}]. To this solution was then added NaN_3 (0.065 g, 1 mM) and air was bubbled through the reaction mixture for 3 h. The final red-brown solution was filtered. Brown crystals of **1** suitable for X-ray analysis were obtained from the filtrate after 72 h. The crystals were filtered off, washed with cold methanol, and dried under vacuum. Yield: 80%. Anal. Calcd for $C_{26}H_{23}CoN_6O_2$ (%): C, 61.18; H, 4.54; N, 16.46. Found: C, 61.08; H, 4.47; N, 16.42. FT-IR (KBr, cm^{-1}): υ_{max}: 2026 (s, N=N=N–), 1620 (s, C=N). UV–Vis (acetonitrile): λ_{max} (nm) (ε, L mol^{-1} cm^{-1}): 640 (200), 432 (6120), 407 (7100), 313 (26,050).

2.2.3. Synthesis of [Co{(naph)$_2$dpt}(N$_3$)] (2). To a stirring solution of $Co(CH_3COO)_2{\cdot}4H_2O$ (249 mg, 1 mM) in methanol (25 mL) was added an equimolar amount of the $H_2(naph)_2dpt$ (439 mg, 1 mM). The pink solution turned brown immediately due to formation of [Co^{II}{(naph)$_2$dpt}] complex. To this solution was then added NaN_3 (0.065 g, 1 mM) and air was bubbled through the reaction mixture for 3 h. The final brown solution was filtered. Brown crystals of **2** suitable for X-ray analysis were obtained from the filtrate after 72 h. The crystals were filtered off, washed with cold methanol, and dried under vacuum. Yield: 84%. Anal. Calcd for $C_{28}H_{27}CoN_6O_2CH_3OH$ (%): C, 61.05; H, 5.48; N, 14.73. Found: C, 60.88; H, 5.37; N, 14.6. FT-IR (KBr, cm^{-1}): υ_{max}: 2033 (s, N=N=N–), 1620 (s, C=N). UV–Vis (acetonitrile): λ_{max} (nm) (ε, L mol^{-1} cm^{-1}): 670 (195), 405 (7400), 304 (36,660).

2.3. *Crystal structure determination*

2.3.1. X-ray crystallography for 1. Brown crystals of **1** suitable for X-ray crystallography were grown by slow evaporation of a methanolic solution at room temperature. Bragg-intensities of **1** were collected at $T = 292$ K on a Stoe IPSD II diffractometer with graphite-monochromated MoKα ($\lambda = 0.71073$ Å) radiation. Cell refinement, data reduction, and a numerical absorption correction were performed with XRED32 (1.31) [16]. The structure was solved with direct methods using SIR2004 [17] and structure refinement on F^2 was carried out with SHELXL [18]. The crystallographic and refinement data are summarized in table 1.

Table 1. Crystal data and structure refinement for **1** and **2**.

Compound	1	2
Empirical formula	$C_{26}H_{23}CoN_6O_2$	$C_{28}H_{27}CoN_6O_2$
Formula weight	510.43	570.53
Temperature (K)	292	100(2)
Crystal system	Monoclinic	Monoclinic
Space group	$P2_1/c$	$P2_1/c$
a (Å)	13.0533(5)	13.2193(2)
b (Å)	12.7672(6)	12.9697(1)
c (Å)	14.6786(6)	15.1460(2)
β (°)	115.811(3)	91.261(1)
V (Å^3)	2202.21(15)	2596.16(6)
Z	4	4
D_{Calcd} (g/cm^3)	1.540	1.460
μ (mm^{-1})	0.818	0.705
Crystal size (mm)	$0.17 \times 0.27 \times 0.8$	$0.30 \times 0.48 \times 0.59$
F(000)	1056	1192
θ Ranges (°)	1.73–29.33	2.07–30.0
Index ranges	$-17 \leqslant h \leqslant 17$, $-17 \leqslant k \leqslant 17$, $-18 \leqslant l \leqslant 20$	$-15 \leqslant h \leqslant 18$, $-17 \leqslant k \leqslant 18$, $-21 \leqslant l \leqslant 21$
Absorption correction	Integration	Multi-scan
Reflections collected	20,692	38,296
Independent reflections (R_{int})	5879 (0.1130)	7537 (0.0198)
Maximum and minimum transmission	0.5864, 0.8994	0.73, 0.82
Data/restraints/parameters	5879/0/316	7537/0/358
Goodness-of-fit on F^2	1.041	1.037
Final R indices [$I > 2\sigma(I)$]	$R_1 = 0.0400$, $wR_2 = 0.0862$	$R_1 = 0.0378$, $wR_2 = 0.0985$
R indices (all data)	$R_1 = 0.0530$, $wR_2 = 0.0934$	$R_1 = 0.0407$, $wR_2 = 0.1012$
Largest diff. peak and hole (e Å^{-3})	0.72 and −0.42	0.94 and −0.69

2.3.2. X-ray crystallography for 2. Brown crystals of **2** suitable for X-ray crystallography were grown by slow evaporation of a methanolic solution at room temperature. Bragg-intensities of **2** were collected at $T = 100$ K on a Bruker APEX-II CCD diffractometer with graphite-monochromated MoKα radiation ($\lambda = 0.71073$ Å). Cell refinement and data reduction were performed with SAINT [19]. Corrections for absorption were carried out with the multi-scan method in SADABS [20]. The structures were solved with direct methods using SHELXS-97 and structure refinement on F^2 was carried out with SHELXL-97 [21]. The crystallographic and refinement data are summarized in table 1.

3. Results and discussion

3.1. *Synthetic study*

Two new cobalt(III) complexes were prepared through oxidation of [Co^{II}{$(naph)_2$dien}] or [Co^{II}{$(naph)_2$dpt}] in the presence of NaN_3. A vigorous stream of air was passed through a solution of the cobalt(II) complexes in methanol for 3 h. Brown crystals of these complexes were obtained in good yield, 80% for **1** and 84% for **2**.

3.2. *Description of structures*

For comparison, we have chosen two complexes from our previous work [13] and labeled them as (**1′**), [Co{$(Me\text{-}sal)_2$dien}(N_3)] and (**2′**), [Co{$(Me\text{-}sal)_2$dpt}(N_3)].

3.2.1. [Co{$(naph)_2$dien}(N_3)] (1). The molecular structure and atom numbering scheme of **1** is presented in figure 1. Crystallographic data and structure analysis for **1** are summarized in table 1. Selected bond distances and angles are given in table 2. The complex

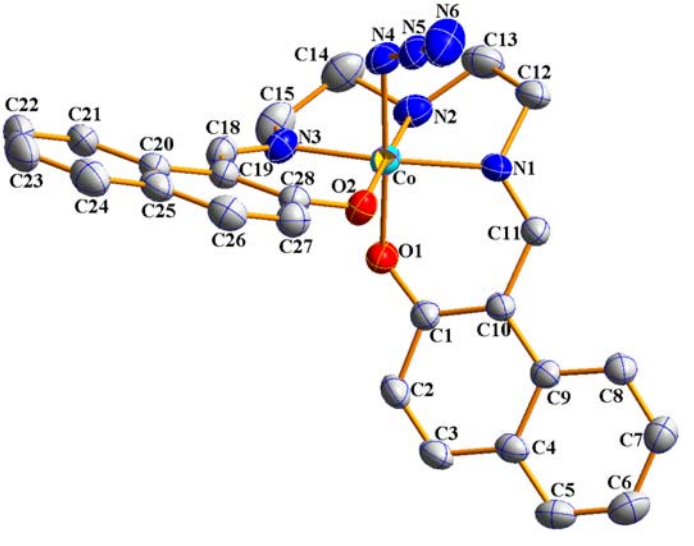

Figure 1. ORTEP-style diagram (50% probability level) of [Co^{III}{$(naph)_2$dien}(N_3)] (**1**) (hydrogens omitted) with atom numbering scheme [30].

Table 2. Selected bond lengths (Å) and angles (°) for **1** and **2**.

	Complex **1**	Complex **2**
Bond lengths		
Co–N1	1.9179(15)	1.9216(11)
Co–N2	1.934(2)	1.9842(11)
Co–N3	1.8778(16)	1.9355(11)
Co–N4	1.9677(16)	1.9593(11)
Co–O1	1.9042(12)	1.9061(9)
Co–O2	1.8775(15)	1.8985(10)
N4–N5	1.195(2)	1.2007(15)
N5–N6	1.154(2)	1.1596(16)
Bond angles		
O1–Co–N1	89.84(5)	89.62(4)
N1–Co–N2	80.18(7)	88.61(5)
N2–Co–N3	87.22(8)	94.78(5)
O2–Co–N3	94.10(7)	89.39(4)
O1–Co–O2	90.92(6)	92.01(4)
O1–Co–N2	87.98(6)	85.99(4)
O1–Co–N4	177.05(7)	177.45(4)
O2–Co–N1	98.52(6)	87.19(4)
O2–Co–N4	89.66(7)	90.17(4)
N1–Co–N3	167.23(8)	176.47(5)
N2–Co–N4	90.07(8)	91.94(5)
N3–Co–N4	89.10(7)	89.05(5)
O1–Co–N3	87.98(6)	89.65(4)
O2–Co–N2	178.66(6)	175.36(5)
N1–Co–N4	92.94(6)	91.82(5)
N4–N5–N6	176.6(2)	175.95(13)

crystallizes in monoclinic space group $P2_1/c$ as a distorted octahedron. Similar to **1′**, in **1** two oxygens are *cis* and the three nitrogens span meridionally. From the three *trans* angles, two {O1–Co1–N4, 177.05(7)° and O2–Co1–N2, 178.66(6)°} are close to ideal and the other {N1–Co1–N3, 167.23(8)°} deviates significantly. The two chelate bite angles formed by the two imine-N and the secondary amine-N of the Schiff base {N1–Co1–N2, 80.18(7)°; N2–Co1–N3, 87.22(8)°} are not identical. Similarly, the six-membered chelate rings formed by phenolate-O and imine-N have different bite angles {O1–Co1–N1, 89.84 (5)°; O2–Co1–N3, 94.10(7)°}.

The crystal of **1** is stabilized by three intermolecular forces as shown in figure 2. (1) Intermolecular hydrogen bonds between the secondary NH_{amine} of one molecule and N_{azido} (N6) of a neighboring molecule {N2–H···N6, 2.489 and N2···N6, 3.207 Å}. (2) C–H···π(C) interactions, i.e. the weakest hydrogen bonds occurring between the soft acid CH and a soft base π-system [22]; our values 2.65–2.74 Å lie within the accepted range [22–24]. The C–H bond points towards the center of an aromatic ring and the angle between the C–H bond and the center of the aromatic ring is close to linear as indicated by the C–H···π lengths and angles presented in table 3. (3) Weaker C–H···N hydrogen bond interactions with shortest C···N distances of 2.92–3.37 Å are in agreement with values reported [25, 26].

3.2.2. [Co{(naph)$_2$dpt}(N$_3$)] (2). The ORTEP diagram of **2** with the atom numbering scheme is shown in figure 3. Selected bond lengths and angles are listed in table 2. The

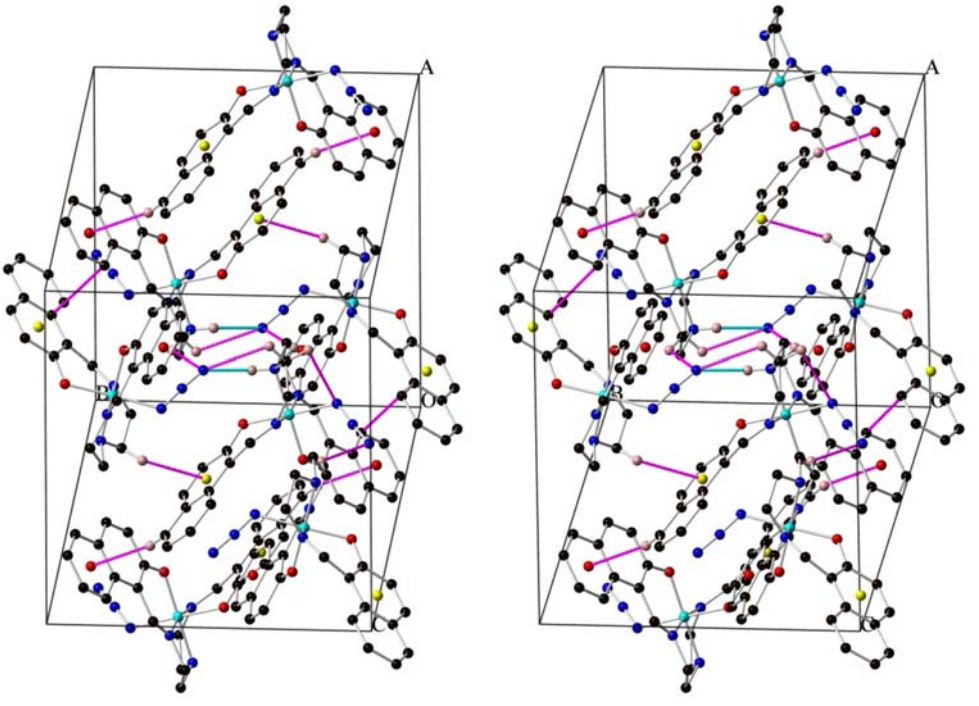

Figure 2. Stereoscopic view of the hydrogen bonds (turquois tubes) and C–H···π(C) interactions (pink tubes) in **1** (see http://dx.doi.org/10.1080/00958972.2013.781159 for color version).

Table 3. Hydrogen bond and C–H···π interactions: lengths (Å) and angles (°) for **1**.

No	D–H···A	D–H (Å)	H···A (Å)	D···A (Å)	D–H···A (°)
1	N2–H2 N···N6$^{(i)}$	0.893	2.489	3.207	137.71
2	C13–H13A···Centroid$^{a(i)}$	0.97	2.738	3.566	143.68
3	C5–H5···Centroid$^{b(i)}$	0.93	2.655	3.540	159.28
4	C13–H13A···N4	0.97	2.733	2.926	91.67
5	C13–H13B···N6$^{(i)}$	0.97	2.742	3.234	112.11
6	C15–H15A···N6$^{(ii)}$	0.97	2.742	3.375	123.52

[a]The distance C–H··· center of the aromatic ring {C1, C2, C3, C4, C9, C10}.
[b]The distance C–H··· center of the aromatic ring {C20, C21, C22, C23, C24, C25}.
Symmetry codes: (i) $1-x, -1/2+y, 1/2-z$; (ii) $x, 1/2-y, -1/2+z$.

octahedral coordination of Co(III) is slightly distorted. From the three *trans* angles, one {O1–Co1–N4, 177.45(4)°} is close to ideal and the other two {N1–Co1–N3, 176.47(5)°} and {O2–Co1–N2, 175.36(5)°} deviate slightly. The two chelate bite angles formed by the two imine-N and the secondary amine-N of the Schiff base {N1–Co1–N2, 88.61(5)°; N2–Co1–N3, 94.78(5)°} are not identical. On the contrary, the six-membered chelate rings formed by phenolate-O and imine-N have similar bite angles {O1–Co1–N1, 89.62(4)°; O2–Co1–N3, 89.39(4)°}.

The coordinating atoms in all four complexes **1′**, **2′** [14], **1**, and **2** are N_4O_2, with the N_{imine}–N_{amine}–N_{imine} of the Schiff base spanning meridionally. The conformations adopted

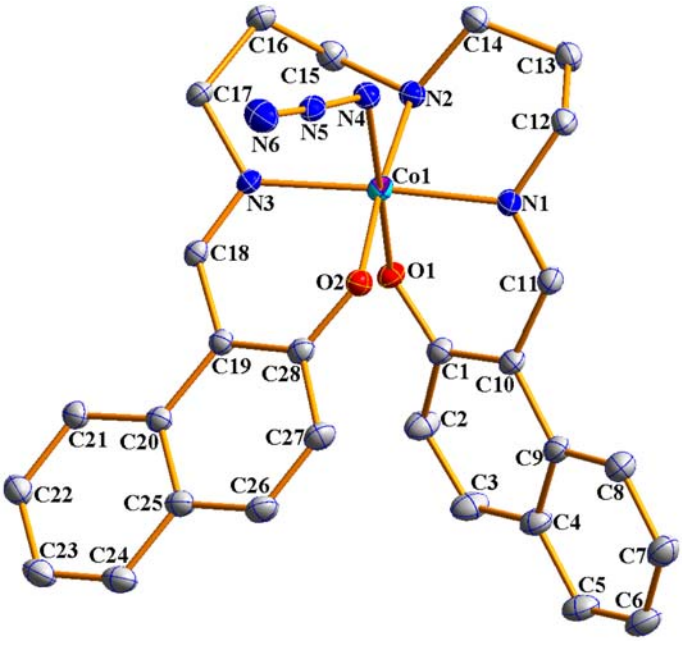

Figure 3. ORTEP-style diagram (50% probability level) of $[Co^{III}\{(naph)_2dpt\}(N_3)]$ (**2**) (hydrogens omitted) with atom numbering scheme [30].

by (Me–sal)$_2$dien and (naph)$_2$dien in **1′** and **1** are similar; however, the conformation adopted by (Me–sal)$_2$dpt in (**2′**) is different from that of (naph)$_2$dptin (**2**). While the two oxygens of (Me–sal)$_2$dpt are *trans* in **2′**, in **2** they are *cis*. These structural differences also manifest their effects in the spectral and electrochemical properties of the two complexes.

The crystal packing of **2** is stabilized by three types of intermolecular forces similar to **1**, as shown in figure 4. (1) Relatively strong intermolecular hydrogen bonding (table 4) between the secondary NH_{amine} of one molecule and N_{azido} (N6) of a neighboring molecule {N2–H···N6, 2.304 and N2···N6, 3.039 Å}. The neutral complexes are linked by N2–H···N6 hydrogen bonds into [001]-chains. A second intermolecular hydrogen bond also exists between O2 of one molecule and hydroxyl of methanol {O3–H3A···O2, 1.97 and O3···O2, 2.806 Å} in the crystal packing of **2**. (2) C–H···π(C) interactions with the intermolecular distances of 2.66–2.95 Å. (3) Weaker C–H···N hydrogen bond interactions with C···N distances of 3.51–3.58 Å.

3.3. *Spectroscopic properties*

Infrared bands were assigned by comparing spectra of the free Schiff bases [14] and those of their cobalt(III) complexes. Two main features are observed in IR spectra of **1** and **2**. (i) A strong absorption at 1620 cm^{-1} for **1** and 1619 cm^{-1} for **2** is assigned to ν(C=N) of imine. These bands appear at lower frequencies relative to the corresponding free Schiff bases, H$_2$(naph)$_2$dien (1633 cm^{-1}) and H$_2$(naph)$_2$dpt (1631 cm^{-1}) upon coordination of the azomethine. (ii) A strong, sharp stretch at 2026 and 2033 cm^{-1} for **1** and **2**, respectively, correspond to the coordinated terminal azide.

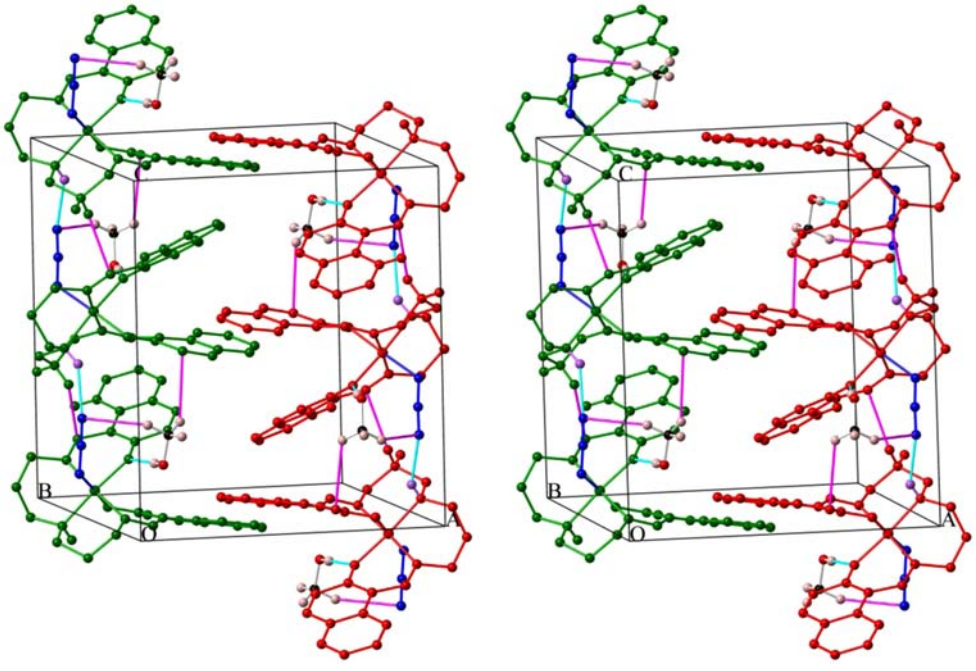

Figure 4. Stereoscopic view of the hydrogen bonds (turquois tubes) and C–H···π(C) interactions (pink tubes) in **2** along the *c* axis (see http://dx.doi.org/10.1080/00958972.2013.781159 for color version).

Table 4. Hydrogen bonds and C–H···π interactions: lengths (Å) and angles (°) for **2**.

No.	D–H···A	D–H (Å)	H···A (Å)	D···A (Å)	D–H···A (°)
1	N2–H2 N···N6$^{(i)}$	0.868	2.304	3.039	142.53
2	C21–H21···N6$^{(ii)}$	0.95	2.619	3.540	163.51
3	C18–H18···N6$^{(ii)}$	0.95	2.640	3.573	167.36
4	C13–H13A···N4$^{(iii)}$	0.99	2.717	3.508	137.19
5	C13–H13A···N5$^{(iii)}$	0.99	2.673	3.587	153.53
6	C13–H13B···C18$^{(i)}$	0.99	2.662	3.422	133.73
7	C3–H3···C3$^{(iv)}$	0.95	2.857	3.257	106.56
8	C29–H29B···N6$^{(v)}$	0.98	2.843	3.674	143.123
9	C29–H29A···C2$^{(v)}$	0.98	2.950	3.581	123.074
10	O3–H3A···O2$^{(i)}$	0.84	1.97	2.806	173.705

Symmetry codes: (i) x, $3/2-y$, $-1/2+z$; (ii) $-x$, $-1/2+y$, $3/2-z$; (iii) $-x$, $2-y$, $1-z$; (iv) $1-x$, $1-y$, $1-z$; (v) x, $3/2-y$, $1/2+z$.

The electronic absorption spectrum of $H_2(naph)_2dien$ in dichloromethane consists of two intense bands at 233 and 308 nm, assigned to $\pi \rightarrow \pi^*$ transitions of the naphthalene rings and azomethine, respectively, and two bands at 403 and 419 nm, corresponding to $n \rightarrow \pi^*$ which, upon coordination of the ligand, disappear. The electronic absorption spectrum of **1** shows, in addition to the intraligand transitions in the UV region, charge-transfer bands at 407 and 432 nm and a band in the visible region at 670 nm corresponding to a $d \rightarrow d$ transition. The electronic absorption spectrum of $H_2(naph)_2dpt$ in dichloromethane shows features similar to those of $H_2(naph)_2dien$, with two $\pi \rightarrow \pi^*$ transitions at 232 and 306 nm,

Table 5. Mean diameter of zone of inhibition (cm) for the antimicrobial activity of **1** and **2**.

Compound	*B. licheniformis*	*S. aureus*
$[Co\{(naph)_2dien\}(N_3)]$ (**1**)	1.7	None
$[Co\{(naph)_2dpt\}(N_3)]$ (**2**)	None	1.5
Penicillin	0.7	0.4

and two $n \rightarrow \pi^*$ transitions at 403 and 421 nm. The $n \rightarrow \pi^*$ bands are absent in the spectrum of the cobalt complex. A charge transfer and a $d \rightarrow d$ transition appear at 405 and 670 nm.

The $d \rightarrow d$ transition for **1** and **2** appears at the same wavelength (670 nm) due to similarity in their molecular structures as discussed in X-ray diffraction section. On the contrary, the d–d transition of **2′** appears at shorter wavelength relative to that of **1′** by ~70 nm [13] because of their structural differences. This structural effect has been confirmed by the electrochemical studies (*vide infra*).

3.4. *Electrochemical studies*

Cyclic voltammograms of **1** and **2** were obtained at 25 °C under argon using acetonitrile solution containing 0.1 M TBAH as supporting electrolyte and complex concentrations of 4×10^{-3} M. The ligands are electro-inactive over a range of +0.8–2.2 V. Redox properties of Co(III) complexes exhibit similar features consisting of an irreversible Co^{III}/Co^{II} reduction at ca. −0.8 V for **1** and **2** (Supplementary material), followed by a chemical reaction. The reduction process of Co(III) complex is accompanied by loss of N_3^- presumably due to the addition of one electron to the antibonding dz^2 orbital [13, 27].

$$[Co^{III}(L)(N_3)] + e \longrightarrow [Co^{II}(L)] + N_3^-$$

In the reverse process, the solvated Co(II) species is reoxidized to Co(III) at much higher potentials (ca. −0.15 V). The appearance of a new reduction wave in the second cycle at less negative potentials indicates that the electron transfer in the first reduction step is followed by a chemical reaction.

The effect of the fused phenyl rings of the two Schiff base ligands on the redox potential of cobalt is evident from the electrochemical data and a comparison with the data obtained for related complexes [13]. These data show that $Co^{III/II}$ reduction in **1** and **2** occurs at more positive potentials relative to **1′** and **2′**. For example, the reduction potentials of **1** and **1′** are −0.793 and −0.951 V ($\Delta E = 158$ mV), respectively. This can be attributed to the electron withdrawing effect by the fused phenyl rings in $(naph)_2$dien.

We have previously demonstrated [13] that Co(III)–Co(II) reduction occurs at more positive potentials in **1′** relative to **2′**. Deviation of the coordination angles from ideal for an octahedral structure (90°) is more pronounced in **1′** than **2′**, rendering the cobalt center more electron deficient in **1′**, and in turn, the reduction occurs at a more positive potential. The observation of the Co(III)–Co(II) reduction peak at ca. −0.8 V for **1** and **2** is presumably due to similarity in the molecular structures and electron density on the metal center in the two complexes and conforms to the energy of the ligand field transition observed in their electronic absorption spectra.

3.5. *Antibacterial activity*

Antibacterial activities of the complexes were tested by the well-known diffusion method using Sabouraud dextrose agar and Müller Hinton agar [28]. The zone of inhibition was recorded on completion of the incubation and the mean diameter for each complex at $100\,\mu g\,mL^{-1}$ was recorded (the Mean Zone of Inhibition is shown in Supplementary Material)v. Stock solutions of **1** and **2** were prepared in DMSO. The diameters of the zone of inhibition produced by the compounds were compared with the standard disk having Penicillin concentration of 10 units per disk. Each test was carried out three times to minimize the error.

The two complexes were subjected to antibacterial activity against Gram-positive *Staphylococcus aureus* and *Bacillus licheniformis*. The screening results are summarized in table 5. It is evident that both complexes have stronger activities than those of the standard antibiotic Penicillin [29].

4. Conclusion

We prepared two new azide cobalt(III) complexes with pentadentate Schiff-base ligands (**1** with $(naph)_2$dien and **2** with $(naph)_2$dpt); they were characterized by elemental analysis, IR spectroscopy, X-ray diffraction, and cyclic voltammetry, and their biological activity was assessed. A comparison with the Me–sal analogs **1′** and **2′** reveals the effect of the disposition of the donors and the ensuing strain on the packing and spectro-electrochemical properties of these complexes. The coordination octahedra are more distorted in **1**, **2** and **1′** relative to **2′**. This can be explained by less structural strain and more efficient overlap between the ligand donor orbitals and the d-orbitals of cobalt that increases electron density on the metal center. Both complexes owe their stability to moderately strong N_{amine}–H$\cdots N_{azide}$ hydrogen bonds, and in the case of **2** also to quite strong $O_{methanol}$–H$\cdots$O hydrogen bonds. The crystal, 3-D in **1** and [001]-chains in **2**, is completed by a multitude of C–H$\cdots\pi$ and $\pi\cdots\pi$ interactions. The electron-withdrawing effect of the fused phenyl rings in naphthaldimine renders Co(III) more easily reducible such that the $[Co^{III}(L)(N_3)] + e \rightarrow [Co^{II}(L)] + N_3^-$ reduction occurs at less negative potentials relative to their Me–salicylidimine-base analogs. An *in vitro* antimicrobial test, with respect to Gram-positive *S. aureus* and *B. licheniformis*, revealed that both complexes have stronger activities than those of Penicillin.

Supplementary material

Crystallographic data for the structural analysis has been deposited with the Cambridge Crystallographic Data Center, CCDC No. 896070 (1) and CCDC No. 896071 (2). These data can be obtained free of charge from www.ccdc.cam.ac.uk/data_request/cif, the Cambridge Crystallographic Data Center.

Acknowledgement

Partial support of this work by the Isfahan University of Technology Research Council is gratefully acknowledged.

References

[1] O.M. Yaghi, H. Li, C. Davis, D. Richardson, T.L. Groy. *Acc. Chem. Res.*, **31**, 474 (1998).
[2] A.C. Grimsdale, K.L. Chan, R.E. Martin, P.G. Jokish, A.B. Holmes. *Chem. Rev.*, **109**, 897 (2009).
[3] J. Otsuky, T. Akasaka, K. Araki. *Coord. Chem. Rev.*, **252**, 32 (2008).
[4] S.S. Tandon, S.D. Bunge, R. Rakosi, Z. Xu, L.K. Thompson. *Dalton Trans*., 6536 (2009).
[5] A. Coleman, M.T. Pryce. *Inorg. Chem.*, **47**, 10980 (2008).
[6] P.A. Vigato, S. Tamburini, L. Bertolo. *Coord. Chem. Rev.*, **251**, 1311 (2007).
[7] J. Ribas, A. Escuer, M. Monfort, R. Vicente, R. Cortes, L. Lezana, T. Rojo. *Coord. Chem. Rev.*, **193–195**, 1027 (1999).
[8] A.F. Knowles, A.K. Nagy. *Eur. J. Biochem.*, **262**, 349 (1999).
[9] R.Y. Li, X.Y. Wang, T. Liu, H.B. Xu, F. Zhao, Z.M. Wang, S. Gao. *Inorg. Chem.*, **47**, 8134 (2008).
[10] A.D. Khalaji, M. Amirnasr, S. Triki. *Inorg. Chim. Acta*, **362**, 587 (2009).
[11] C. Adhikary, S. Koner. *Coord. Chem. Rev.*, **254**, 2933 (2010).
[12] S. Meghdadi, K.J. Schenk, M. Amirnasr, F. Fadaee. *Acta Crystallogr.*, **E64**, m479 (2008).
[13] S. Meghdadi, K. Mereiter, M. Amirnasr, F. Fadaee, A. Amiri. *J. Coord. Chem.*, **62**, 734 (2009).
[14] M. Amirnasr, F. Fadaee, K. Mereiter. *Inorg. Chim. Acta*, **371**, 6 (2011).
[15] N.G. Connelly, W.E. Geiger. *Chem. Rev.*, **96**, 877 (1996).
[16] X-RED32. *Version 1.31*, Stoe & Cie GmbH, Germany (2005).
[17] M.C. Burla, R. Caliandro, M. Camalli, B. Carrozzini, G.L. Cascarano, L. De Caro, C. Giacovazzo, G. und R. Polidori Spagna, *SIR2004: J. Appl. Cryst*., **38**, 381 (2005).
[18] G.M. Sheldrick. *Acta Cryst.*, **A64**, 112 (2008).
[19] Bruker AXS. *Programs SMART, version 5.626; SAINT, version 6.36A; XPREP, version 6.12*, Madison, Wiskonsin, USA (2001).
[20] G.M. Sheldrick. *SADABS: Program for Empirical Absorption and Other Corrections*, University of Göttingen, Germany (1997).
[21] G.M. Sheldrick. *SHELX97: Program System for Crystal Structure Determination*, University of Göttingen, Germany (1997).
[22] M. Nishio. *Cryst. Eng. Commun.*, **6**, 130 (2004).
[23] S. Harder. *Chem. Eur. J.*, **5**, 1852 (1999).
[24] E.A. Meyer, R.K. Castellano, F. Diederich. *Angew. Chem. Int. Ed.*, **42**, 1210 (2003).
[25] Z. Berkovitch-Yellin, L. Leiserowitz. *Acta Cryst.*, **B40**, 159 (1984).
[26] L.M. Fitzsimons, J.F. Gallagher. *Acta Cryst.*, **C55**, 472 (1999).
[27] A. Bottcher, T. Takeuchi, K.I. Hardcastle, T.J. Meade, H.B. Gray. *Inorg. Chem.*, **36**, 2498 (1997).
[28] S. Magaldi, S. Mata-Essayag, C.H. de Capriles, C. Perez, M.T. Colella, C. Olaizola, Y. Ontiveros. *Int. J. Infect. Dis.*, **8**, 39 (2004).
[29] H.C. Zahid. *Appl. Organomet. Chem.*, **16**, 17 (2002).
[30] vK. Brandenberg, H. Putz. Diamond - Crystal and Molecular Structure Visualization, Crystal Impact, Kreuzherrenstraße 102, D-53227 Bonn, Germany.